Can porosity affect the hyperspectral signature of sandy landscapes?

Gladimir V. G. Baranoski, Bradley W. Kimmel

Can porosity affect the hyperspectral signature of sandy landscapes?

Gladimir V. G. Baranoski and Bradley W. Kimmel

Natural Phenomena Simulation Group, School of Computer Science, University of Waterloo, 200 University Avenue West, Waterloo, Canada

ABSTRACT

Porosity is a fundamental property of sand deposits found in a wide range of landscapes, from beaches to dune fields. As a primary determinant of the density and permeability of sediments, it represents a central element in geophysical studies involving basin modeling and coastal erosion as well as geoaccoustics and geochemical investigations aiming at the understanding of sediment transport and water diffusion properties of sandy landscapes. These applications highlight the importance of obtaining reliable porosity estimations, which remains an elusive task, notably through remote sensing. In this work, we aim to contribute to the strengthening of the knowledge basis required for the development of new technologies for the remote monitoring of environmentally-triggered changes in sandy landscapes. Accordingly, we employ an *in silico* investigation approach to assess the effects of porosity variations on the reflectance of sandy landscapes in the visible and near-infrared spectral domains. More specifically, we perform predictive computer simulations using SPLITS, a hyperspectral light transport model for particulate materials that takes into account actual sand characterization data. To the best of our knowledge, this work represents the first comprehensive investigation relating porosity to the reflectance responses of sandy landscapes. Our findings indicate that the putative dependence of these responses on porosity may be considerably less pronounced than its dependence on other properties such as grain size and shape. Hence, future initiatives for the remote quantification of porosity will likely require reflectance sensors with a high degree of sensitivity.

Keywords: sand, porosity, water saturation, sphericity, roundness, reflectance, predictive simulations, controlled experiments.

1. INTRODUCTION

Soil samples are composed of particles (grains) of weathered rock and sometimes organic matter immersed in a medium of air and water (the pore space).[1] They are classified according to the size distribution of the mineral particles.[2] This is accomplished first by assigning individual particles to classes, called soil separates, according to their size. Various agencies have differing definitions for soil separates and textural classes In this work, we use the system developed by the United States Department of Agriculture (USDA).[3] The USDA defines three soil separates, called sand, silt, and clay. After soil particles are divided into these classes, from the largest to the smallest particles, respectively,[4] the relative masses of each soil separate are then compared to determine the texture of a soil sample. A sand-textured soil, henceforth referred to as sand soil or sand deposit, contains at least 85% sand-sized particles.[3]

The porosity of a soil sample corresponds to the volume of the pore space as a fraction of the total volume of the sample.[5] It varies with soil texture, however, with coarse soils being less porous than finer soils.[5] For sand-textured soils, porosity typically varies between 35% and 50%,[2,6] albeit one can find values as low as 19.6%[7] and as high as 66%[8] in the literature.

Porosity is a primary determinant of the density and permeability of sediments. It represents a vital input for basin modeling and studies involving coastal erosion.[6] Moreover, the porosity of a sand deposit can be used to calculate its wet bulk density.[9] This quantity, in turn, is of interest for a variety of geoaccoustics[10] and biogeochemical[9] investigations aiming at the understanding of sediment transport and water diffusion properties

Further author information: (Send correspondence to Gladimir V. G. Baranoski)
Gladimir V. G. Baranoski: E-mail: gvgbaran@cs.uwaterloo.ca

Earth Resources and Environmental Remote Sensing/GIS Applications VIII, edited by Ulrich Michel, Karsten Schulz
Proc. of SPIE Vol. 10428, 104280S · © 2017 SPIE · CCC code: 0277-786X/17/$18 · doi: 10.1117/12.2278683

of sandy landscapes. This connection between porosity and water flow is also one of the focal points of hydrological studies involving the permeability of aquifers.[9]

These applications underscore the importance of obtaining reliable porosity estimations. Accordingly, different techniques have been proposed for obtaining *in situ* samples of sand deposits from which porosities can be measured. These techniques, however, have been often undermined by grain breakage and core disturbance problems.[7,9,10] More recently, non-destructive approaches, such as the nuclear densimeter method,[6] are being proposed to eliminate the physical handling of the sand samples, which can disturb their loosely packed grains, and enable repetitive measurements at a single test location. When it comes to the remote estimation of this property, however, there is still a long way to go in view of the relative scarcity of studies relating soil optical properties to porosity,[11,12] particularly with respect to sand deposits.[13] In order to determine the feasibility of initiatives aimed at the remote quantification of this property, we believe that it is necessary to examine these relationships more closely. These aspects have motivated the research presented in this paper.

In this work, we investigate the effects of porosity on the hyperspectral signatures of sandy landscapes. Our primary goal is to assess the putative dependence of these signatures on the porosity of these terrains, which can affect the feasibility of initiatives aimed at the remote quantification of this soil property. In order to overcome the difficulties inherent to *in situ* studies, we employ an *in silico* approach. More specifically, we perform predictive computer simulations using a hyperspectral model for particulate materials, known as SPLITS (*Sp*ectral *Li*ght *T*ransport Model for *S*and),[13] which takes into account actual sand characterization data. Through this approach, we can perform controlled experiments on sand samples, *i.e.*, we can assign different values to specific parameters and analyze their effects on the samples' hyperspectral responses while keeping the other parameters constant. We remark that such controlled experiments are difficult to perform effectively under actual laboratory conditions. Our findings are expected to strengthen the knowledge basis to be used in the development of new high-precision technology for the monitoring of environmentally-triggered changes in sandy landscapes associated with porosity variations.

2. INVESTIGATION FRAMEWORK

Our investigation is focused on surficial, noncemented sand deposits. Besides variations on porosity (P), it takes into account variations on other sand properties, namely the degree of saturation, grain size and shape.[13] The degree of saturation (S) corresponds to fraction of pore space occupied by water. The shape of a grain is usually defined by two parameters: roundness (R) and sphericity (Ψ).[14] While roundness can be described as the measure of detail in the features on the grain surface, sphericity refers to the degree to which the grain approaches a spherical shape.[15]

In our investigation, we also consider different iron-oxide distribution patterns within the samples. Iron oxides, such as hematite, goethite and magnetite, may occur as pure particles,[16] as contaminants mixed with the parent material,[17] or as coatings, within a kaolinite or illite matrix, formed on the grains during wind transport.[18] In terrestrial sand soils, the parent material is typically a material like quartz or calcite, with quartz (employed in this investigation) being the most common.[19]

As the baseline references for our investigation, we employ directional-hemispherical reflectance curves (over the 400 to 1000 nm region) computed for two selected sand samples with distinct morphological and mineralogical characteristics using SPLITS. The actual reflectance curves measured for these samples[20] were made available in the U.S. Army Topographic Engineering Center (TEC) database.[20] These samples are from a red (hematite-rich) dune in Australia (TEC #10019201) and a magnetite-rich beach site in Peru (TEC #10039240). Based on their descriptions,[20] we assumed that the presence of clay-sized particles and moisture (water content) were negligible in these samples.

For the computation of the modeled curves, besides considering $S = 0$, we employed mean values for the porosity ($P = 42.5\%$), grain roundness ($R = 0.482$) and grain sphericity ($\Psi = 0.798$) found in the literature.[2,14] The remaining model parameter values employed to compute the modeled curves for these samples are given in Table 1. Note that the percentages of the sand-sized and silt-sized particles depicted in Table 1 are used to compute their dimensions during the simulations[15] using a particle size distribution provided by Shirazi *et al.*[4] The corresponding particle dimensions are provided in Table 2.

Model Parameters	Samples	
	Australian Dune	Peruvian Beach
s_a	85	92.8
s_i	15	7.2
μ_p	0	50
μ_m	90	0
μ_c	10	50
r_{hg}	0.75	0.35
ϑ_{hg}	0.01	0.045
ϑ_m	0	0.17

Table 1: Parameters used to obtain the modeled spectral reflectance curves for the Australian and Peruvian TEC samples.[20] The texture of the samples is described by the percentages (%) of sand (s_a) and silt (s_i) particles. The particle type distributions considered in the simulations are given in terms of the percentages (%) of pure (μ_p), mixed (μ_m) and coated (μ_c) grains. It is assumed that magnetite appears as pure particles in sand soils characterized by the presence of this mineral.[21] The parameter r_{hg} corresponds to the ratio between the mass fraction of hematite to the total mass fraction of hematite and goethite represented by ϑ_{hg}. The parameter ϑ_m represents the mass fraction of magnetite.

Fractions		Sand		Silt	
s_a	s_i	d_a	σ_a	d_i	σ_i
0.850	0.150	0.112	2.170	0.173	3.320
0.928	0.072	0.141	2.040	0.401	4.160

Table 2: Geometric mean particle diameters (given in mm) and standard deviations for soils with various mixtures of sand-sized particles (s_a) and silt-sized particles (s_i) considered in our simulations. The diameters and standard deviations for sand-sized particles (d_a and σ_a, respectively) and silt-sized particles (d_i and σ_i, respectively) are provided by Shirazi *et al.*[4] Note that the presence of clay-sized particles is assumed to be negligible in the sand samples considered in this work.

Within the SPLITS' geometrical-optics formulation, light interacting with a given sand sample is represented by rays that can be associated with any wavelength (λ). Hence, SPLITS can provide reflectance curves with different spectral resolutions. For consistency, all modeled curves depicted in this work have a spectral resolution of 5 nm. These curves were obtained using a virtual spectrophotometer.[22] In their computation, we considered 10^6 sample rays and an angle of incidence of 0° for consistency with the actual measurements set-up employed by Rinker *et al.*[13,20]

To enable the full reproduction of our *in silico* experimental results, we made SPLITS available online[23] via a model distribution system.[24] This system enables researchers to specify experimental conditions (*e.g.*, angle of incidence and spectral range) and sand characterization parameters using a web interface,[23] and receive customized simulation results. In addition, the supporting data (*e.g.*, refractive index and extinction coefficient curves) used in our investigation were also made available online.[25]

As it can be observed in the graphs presented in Figure 1, the modeled curves show a close agreement with their measured counterparts. Accordingly, we employed these modeled curves as the control (baseline) curves for our *in silico* experiments involving variations in porosity, degree of saturation, roundness and sphericity. More precisely, the datasets used to generate the baseline curves, with the exception of the values for the parameters associated with these variations, were employed to generate the curves resulting from our experiments. In our simulations, we considered typical lower and upper bounds for P (0.3 and 0.5),[2,6] S (0 and 1), R (0.2 and 0.7)[14] and Ψ (0.6 and 0.95).[14] Note that $R = 0.7$ corresponds to the smoothest grains, while $\Psi = 0.95$ corresponds to grains whose geometry is the closest to that of a sphere.

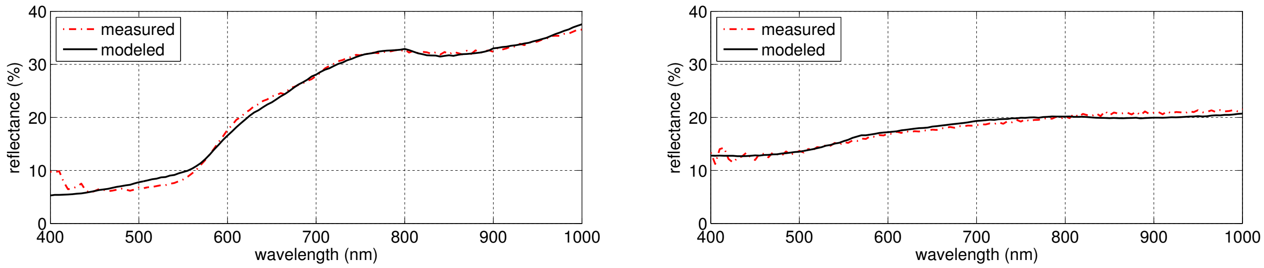

Figure 1: Measured and modeled reflectance curves for the two sand samples employed as baseline references in this investigation. Left: a hematite-rich (red) dune in Australia (TEC #10019201). Right: a magnetite-rich (dark) beach site in Peru (TEC #10039240). The measured curves were obtained from the U.S. Army Topographic Engineering Center (TEC) database.[20] The modeled curves were obtained using the SPLITS model.[13,23]

Finally, in order to quantify the reflectance changes resulting from porosity variations, we compute the mean relative difference between the respective curves for the two spectral regions of interest, namely visible (400-700 nm) and near-infrared (700-1000 nm). This quantity is given in terms of percentage (%) and it is expressed as:

$$MRD = \frac{1}{N}\sum_{i=1}^{N}\frac{|\rho_{P=0.3}(\lambda_i) - \rho_{P=0.5}(\lambda_i)|}{\rho_{P=0.5}(\lambda_i)} \times 100, \tag{1}$$

where $\rho_{P=0.3}$ and $\rho_{P=0.5}$ correspond to the reflectance curves obtained considering porosity set to 0.3 and 0.5, respectively, and N is the total number of wavelengths sampled with a $5nm$ resolution within the selected spectral region.

3. RESULTS AND DISCUSSION

In our first set of experiments, we simulated the combined effects of variations in porosity and degree of saturation on the reflectances of the selected samples. Although the resulting plots depicted in Figure 2 show the expected reflectance reduction associated with the increase in the degree of saturation,[13] they show only minor changes associated with the different porosity values. More specifically, in the case of the Australian dune sample (Figure 2 left), which was modeled considering smaller particle dimensions, one can only observe a minor reflectance reduction from 400 to 950 nm when the porosity is increased from 0.3 to 0.5 and the degree of saturation is set to 0. In addition, one can also observe a minor increase in the reflectance between 950 and 1000 nm under the same conditions. When the degree of saturation is set to 1, the reflectance changes become slightly smaller in the visible region and slightly larger in the near-infrared region. In the case of the Peruvian beach sample (Figure 2 right), which was modeled considering larger particle dimensions, one can observe a minor reflectance reduction along the entire region of interest from 400 to 1000 nm when the porosity is increased from 0.3 to 0.5 and the degree of saturation is set to 0. When it is set to 1, the reflectance changes become slightly larger. This visual inspection of the curves presented in Figure 2 is supported by the corresponding MRD values provided in Table 3.

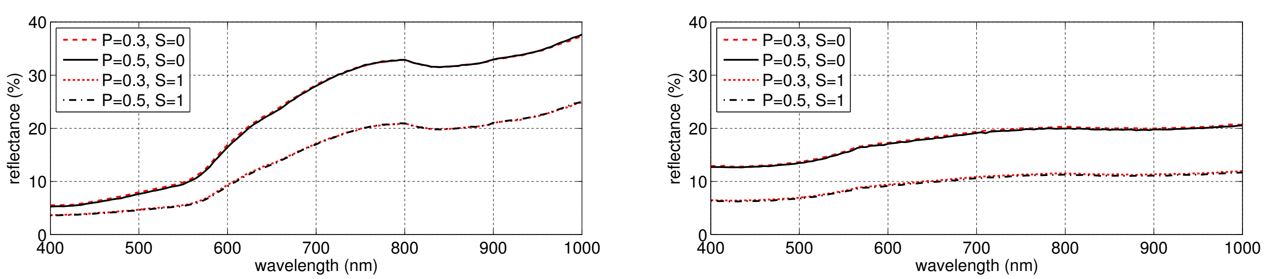

Figure 2: Comparison of modeled reflectance curves considering variations in porosity (P) and degree of saturation (S). Left: Australian dune sample. Right: Peruvian beach sample.

Model Parameter	Australian Dune Visible	Australian Dune Near-Infrared	Peruvian Beach Visible	Peruvian Beach Near-Infrared
$S = 0$	3.17	0.26	1.38	1.24
$S = 1$	2.00	0.34	2.32	2.07

Table 3: Mean relative difference (MRD) values computed for the curves depicted in Figure 2. These values are given in terms of the percentages (%).

In our second set of experiments, we simulated the combined effects of variations in porosity and roundness on the reflectances of the selected samples. Although the resulting plots depicted in Figure 3 show the expected reflectance reduction associated with the increase in roundness,[15] again they show only minor changes associated with the different porosity values. More specifically, in the case of the Australian dune sample (Figure 3 left), one can only observe a minor reflectance reduction, notably in the visible region, when the porosity is increased from 0.3 to 0.5 and the roundness is set to 0.2. When it is set to 0.7, the reflectance changes become slightly smaller in the visible region and slightly larger in the near-infrared region. In the case of the Peruvian beach sample (Figure 2 right), again one can observe a minor reflectance reduction along the entire region of interest from 400 to 1000 nm when the porosity is increased from 0.3 to 0.5 and the roundness is set to 0.2. When it is set to 0.7, the reflectance changes become slightly larger. This visual inspection of the curves presented in Figure 3 is supported by the corresponding MRD values provided in Table 4.

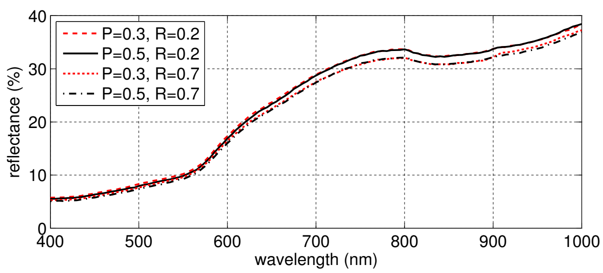

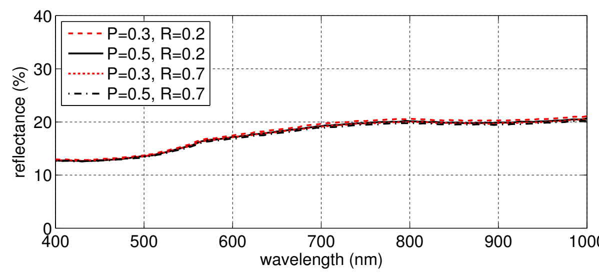

Figure 3: Comparison of modeled reflectance curves considering variations in porosity (P) and roundness (R). Left: Australian dune sample. Right: Peruvian beach sample.

Model Parameter	Australian Dune Visible	Australian Dune Near-Infrared	Peruvian Beach Visible	Peruvian Beach Near-Infrared
$R = 0.2$	3.14	0.27	1.38	2.13
$R = 0.7$	2.86	0.60	1.24	1.14

Table 4: Mean relative difference (MRD) values computed for the curves depicted in Figure 3. These values are given in terms of the percentages (%).

In our third set of experiments, we simulated the combined effects of variations in porosity and sphericity on the reflectances of the selected samples. Similarly to the previous sets of experiments, although the resulting plots depicted in Figure 4 show the expected reflectance changes associated with the variations in sphericity,[15] they show only minor quantitative changes associated with the different porosity values. In this set of experiments, however, we noticed some distinct qualitative trends. In the case of the Australian dune sample (Figure 4 left), while one can observe a minor reflectance reduction in the region from 400 to ≈620 nm when the porosity is increased from 0.3 to 0.5 and the sphericity is set to 0.6, one can observe a minor reflectance increase in the region from ≈620 to 1000 nm. When the sphericity is set to 0.95, however, one can observe a reflectance reduction along the entire region of interest. In the case of the Peruvian beach sample (Figure 4 right), one can observe a minor reflectance reduction in the region from 400 to ≈490 nm and a minor reflectance increase from ≈490 to 1000 nm when the porosity is increased from 0.3 to 0.5 and the sphericity is set to 0.6. When it is set to 0.95, however, one can observe a minor reflectance reduction along the entire region of interest (from 400 to 1000 nm). This visual inspection of the curves presented in Figure 4 is supported by the corresponding MRD values provided in Table 5.

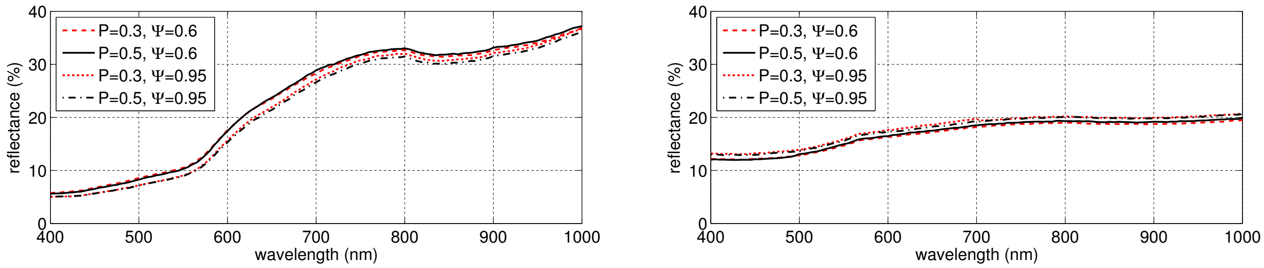

Figure 4: Comparison of modeled reflectance curves considering variations in porosity (P) and sphericity (Ψ). Left: Australian dune sample. Right: Peruvian beach sample.

Model	Australian Dune		Peruvian Beach	
Parameter	Visible	Near-Infrared	Visible	Near-Infrared
$\Psi = 0.6$	2.12	1.15	1.26	1.86
$\Psi = 0.95$	1.39	1.79	1.84	0.54

Table 5: Mean relative difference (MRD) values computed for the curves depicted in Figure 4. These values are given in terms of the percentages (%).

In all tested cases, a 60% variation in porosity resulted in minor reflectance changes, on average below 3.5%. We also note that similar variations in the other sand properties, notably grain size and sphericity, result in significantly larger reflectance changes.[13,15] Considering these aspects, the results of our *in silico* experiments demonstrate that, for sand deposits with typical mineralogical and morphological characteristics, the putative reflectance dependence on porosity[12] is markedly weaker than its dependence on these other properties in the spectral region of interest (from 400 to 1000 nm). Although our findings should be confirmed by actual spectrophotometric experiments, they clearly indicate that new initiatives for the remote detection of porosity variations on sand deposits will require sensors with a high degree of sensitivity. Moreover, since previous works[6,9] have indicated that the permeability of sand deposits may be correlated with grain size and sphericity in addition to porosity, future studies in this area, particularly those supported by remote sensing technologies, should take into account the potential masking effects that reflectance changes due to these properties may have on reflectance changes due to porosity.

4. CONCLUSION AND FUTURE WORK

Although there have been previous works[11,12] relating soil optical properties to porosity, to the best of our knowledge, the research presented in this paper represents the first comprehensive investigation relating porosity and the hyperspectral signature of sand soils. Our *in silico* experiments, which were primarily focused on the assessment of the putative dependence of the hyperspectral reflectance of these media to their porosity, demonstrate that such a dependence may be considerably weaker than originally expected, notably for sand soils with typical mineralogical and morphological characteristics, in the spectral region from 400 to 1000 nm. We believe that our findings, albeit still subjected to further validation through actual spectrophotometric experiments, should be taken into account in the design of new technologies for the remote monitoring of this fundamental soil property.

As future work, we plan to extend our research to the effects of porosity on the spatial distribution of the reflected light. More specifically, we intend to investigate the effects of porosity variations on the bidirectional surface scattering distribution function (BSSDF) of sand soils. We also plan to extend it to extra-terrestrial sand soils characterized by distinct parent materials.

REFERENCES

[1] Gerrard, J., [*Fundamentals of Soils*], Routledge, New York, NY, USA (2000).

[2] Brady, N., [*The Nature and Properties of Soils*], Macmillan Publishing Co., New York, NY, USA, 8th ed. (1974).

[3] Staff, S. S. D., "Soil survey manual," Tech. Rep. USDA Handbook 18, Soil Conservation Service, United States Department of Agriculture (1993).

[4] Shirazi, M., Boersma, L., and Hart, J., "A unifying quantitative analysis of soil texture: Improvement of precision and extension of scale," *Soil Science Society of America Journal* **52**(1), 181–190 (1988).

[5] Brady, N. and Weil, R., [*Elements of the Nature and Properties of Soils*], Prentice-Hall Inc., Upper Saddle River, NJ, USA (2000).

[6] Román-Sierra, J., noz Perez, J. M., and Navarro-Plus, M., "Beach nourishment effects on sand porosity variability," *Coastal Engineering* **83**, 221–232 (2014).

[7] Dickinson, W. and Ward, J., "Low depositional porosity in eolian sands and sandstones, Namib desert," *Journal of Sedimentary Research* **A64**(2), 226–232 (1994).

[8] Jackson, P., Smith, D., and Stanford, P., "Resistivity-porosity-particle shape relationships for marine sands," *Geophysics* **43**, 1250–1268 (1978).

[9] Curry, C., Bennett, R., Hulbert, M., Curry, K., and Faas, R., "Comparative study of sand porosity and a technique for determing porosity of undisturbed marine segment," *Marine Georesources & Geotechnology* **22**, 231–252 (2004).

[10] Tang, D., Briggs, K., Williams, K., Jackson, D., Thorsos, E., and Percival, D., "Fine-scale volume heterogeneity measurements in sand," *Soil Science Society of America Journal* **27**(3), 546–560 (2002).

[11] Manchanda, M., Kudrat, M., and Tiwari, A., "Soil survey and mapping using remote sensing," *Tropical Ecology* **43**(1), 61–74 (2002).

[12] Hapke, B., "Bidirectional reflectance spectroscopy 6. Effects of porosity," *Icarus* **195**, 918–926 (2008).

[13] Kimmel, B. and Baranoski, G., "A novel approach for simulating light interaction with particulate materials: application to the modeling of sand spectral properties," *Optics Express* **15**(15), 9755–9777 (2007).

[14] Vepraskas, M. and Cassel, D., "Sphericity and roundness of sand in costal plain soils and relationships with soil physical properties," *Soil Science Society of America Journal* **51**(5), 1108–1112 (1987).

[15] Baranoski, G., Kimmel, B., Chen, T., and Miranda, E., "Influence of sand-grain morphology and iron-oxide distribution patterns on the visible and near-infrared reflectance of sand-textured soils," *IEEE Journal of Selected Topics in Applied Earth Observations and Remote Sensing* **7**(9), 3755–3763 (2014).

[16] Catling, D. and Moore, J., "The nature of coarse-grained crystalline hematite and its implications for the early environment of Mars," *Icarus* **165**, 277–300 (2003).

[17] Mottana, A., Crespi, R., and Liborio, G., [*Simon and Schuster's Guide to Rocks and Minerals*], Simon and Schuster, Inc., New York, NY, USA (1978).

[18] Wopfner, H. and Twidale, C., "Australian desert dunes: wind rift or depositional origin?," *Australian Journal of Earth Sciences* **48**, 239–244 (2001).

[19] Leu, D., "Visible and near-infrared reflectance of beach sands: a study on the spectral reflectance/grain size relationship," *Remote Sensing of Environment* **6**(3), 169–182 (1977).

[20] Rinker, J., Breed, C., MCCauley, J., and Corl, P., "Remote sensing field guide - desert," Tech. Rep. ETL-0588, U.S. Army Topographic Engineering Center, Fort Belvoir, VA, USA (September 1991).

[21] Hunt, G., Salisbury, J., and Lenhoff, C., "Visible and near-infrared spectra of minerals and rocks: III oxides and hydroxides," *Modern Geology* **2**(3), 195–205 (1971).

[22] Baranoski, G., Rokne, J., and Xu, G., "Virtual spectrophotometric measurements for biologically and physically-based rendering," *The Visual Computer* **17**(8), 506–518 (2001).

[23] Natural Phenomena Simulation Group (NPSG), *Run SPLITS Online*. School of Computer Science, University of Waterloo, Ontario, Canada (2012). `http://www.npsg.uwaterloo.ca/models/splits.php`.

[24] Baranoski, G., Dimson, T., Chen, T., Kimmel, B., Yim, D., and Miranda, E., "Rapid dissemination of light transport models on the web," *IEEE Computer Graphics & Applications* **32**(3), 10–15 (2012).

[25] Natural Phenomena Simulation Group (NPSG), *Sand Data*. School of Computer Science, University of Waterloo, Ontario, Canada (2012). `http://www.npsg.uwaterloo.ca/data/sand.php`.